Chapter 17

Micropipette Aspiration of Oocytes to Assess Cortical Tension

Janice P. Evans and Douglas N. Robinson

Abstract

Just as it is important to understand the cell biology of signaling pathways, it is valuable also to understand mechanical forces in cells. The field of mechanobiology has a rich history, including study of cellular mechanics during mitosis and meiosis in echinoderm oocytes and zygotes dating back to the 1930s. This chapter addresses the use of micropipette aspiration (MPA) to assess cellular mechanics, specifically cortical tension, in mammalian oocytes.

Key words Cellular mechanics, Signaling pathways, Mitosis, Meiosis

1 Introduction

Go suck an egg.

This expression has been used as a disparaging, dismissive comment—but for us, it became a research direction. We teamed up 10 years ago, initially with the goal of testing the hypothesis that the membrane block to polyspermy in mammalian eggs would be associated with a change in cellular mechanics in the oocytes. While our data ultimately were not consistent with this hypothesis that the membrane block to polyspermy was a mechanical block, dependent on a change in cortical mechanics in the early embryo [1, 2], our foray into oocyte cellular mechanics has still been highly fruitful, and paved the way for a body of interesting work by us and others.

In our studies of cellular mechanics in mouse oocytes, we used micropipette aspiration (*MPA*) to assess *cortical tension*, or the force in the cortex and overlying plasma membrane that serves to minimize the surface area to volume ratio [3, 4]. These MPA studies identified dramatic changes in cortical tension in oocytes with progression through meiotic maturation and egg activation, as well as ~threefold mechanical polarity in the metaphase II egg, with higher tension in the spindle-sequestering amicrovillar domain as compared to the microvillar domain, which supports sperm

Marie-Hélène Verlhac and Marie-Emilie Terret (eds.), *Mouse Oocyte Development: Methods and Protocols*, Methods in Molecular Biology, vol. 1818, https://doi.org/10.1007/978-1-4939-8603-3_17,

interaction [1]. Perturbation of cortical tension through disruption of actomyosin or function of the family of actin-to-membrane tethering proteins known as ERMs (family members, *e*zrin, *r*adixin, and *m*oesin) causes significant defects in spindle function during exit from metaphase II arrest upon fertilization [1]. Others (including the editors of this volume) built on this work, and demonstrated that oocyte mechanics must be carefully regulated for spindle migration to the cortex during meiosis I, and if the oocyte cortex is too hard or too soft, the metaphase I spindle does not move to the oocyte periphery [5, 6]. Studies of cortical mechanics have been extended to mouse and human embryos, with data identifying correlation between mechanical parameters and embryo viability and developmental potential [7]. The significance in research into cellular mechanics of oocytes is also highlighted in studies of in vitro oocyte development, with oocytes derived in vitro from primordial germ cell-like cells (PGCLCs) [8]. While some of these oocytes produced offspring, other oocytes had defects with clear relevance cellular mechanics; ~50% of the PGCLC-derived oocytes had "cytoskeletal immaturity/fragility" and failed to emit second polar bodies [8]. We observe the same abnormality in eggs with abnormal cortical tension [1]. This further underscores the importance of cellular mechanics in oocyte function and quality.

Some of the earliest studies of cellular mechanics applied different approaches, including MPA, to echinoderm eggs and embryos [9–15]. MPA can be used to measure a variety of mechanical parameters, including elasticity, viscoelasticity, and cortical tension [16, 17]. While these parameters are interrelated, they are not perfect surrogates for each other. However, cortical tension reflects longer time-scale mechanics and is relevant for the larger scale shape changes, such as those associated with polar body formation, and also is a little easier to standardize for mammalian oocytes. Therefore, we address the measurement of cortical tension by MPA in this chapter.

Cortical tension is a highly sensitive readout of contractility in the cortical cytoskeleton, and reflects the biochemical and structural features of the cortex, which are mediated by actin assembly, myosin-II motor activity, organization of actin polymers, and linkages between the polymers and the membrane [18]. There are other approaches to assess cellular mechanics as well, but MPA has been our method of choice for a variety of reasons. Particle tracking methods (e.g., such as the Robinson lab has used to study *Dictyostelium* amoebas (e.g., [16, 19, 20])) are not particularly well suited to cells as large as oocytes. Atomic force microscopy (*AFM*) is another powerful method, although it is worth noting that AFM typically measures mechanical parameters on shorter submicrometer length-scales while MPA measures mechanics on larger lengths-scales [21]. Thus, the parameters assessed by MPA

are highly relevant for the μm-scale aspects of oocyte biology, such as cell division associated with polar body emission. We have also found that measurements made by micropipette aspiration agree quantitatively with microrheology (which measures very short time-scale mechanics) [19, 20, 22, 23]. Similarly, we have found that elasticity values for breast cancer epithelial cells measured by MPA agree closely with published values from atomic force microscopy [24, 25].

MPA has proved ideal for mechanical measurements of oocytes, being highly amenable to the very large, round, and nonadherent oocytes. MPA allows both elastic and viscous mechanical elements to be quantified, and the parameters measured by MPA are readily applicable for computational work [22, 26]. MPA measures longer time-scale mechanics (>0.5 s), and deforms the cortex over areas of a few tens of μm^2, thus averaging out shorter length-scale mechanics. This is actually a benefit because statistical significance can be achieved with relatively fewer measurements than are needed by AFM or microrheological measurements. In our MPA studies, we have measured an "effective cortical tension" (T_{eff}), measured in units of nN/μm (*see* also **Note 3**). This parameter is measured at a

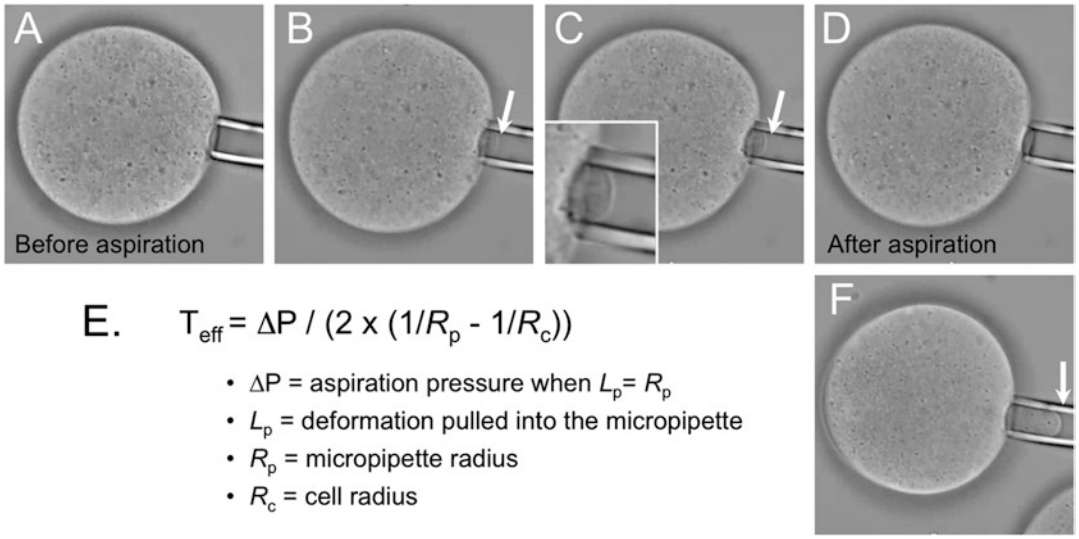

Fig. 1 Panels **a**–**d** show individual images from live-cell imaging of an oocyte subjected to micropipette aspiration (MPA). Panel **c** includes an inset, with a close-up of the cell tether aspirated into the pipette. We calculate effective cortical tension (T_{eff}) as shown in Panel **e**, with the key parameters from analysis of the live-cell imaging being (**a**) pipette radius (R_p in μm), (**b**) equilibrium cortex tether upon aspiration (L_p in μm) when $L_p = R_p$, (**c**) cell radius (R_c in μm). The other key parameter, aspiration pressure (ΔP) comes from notes taken during the live-cell imaging. This value is calculated as $\Delta P = \rho g h$, where ρ is the density of water (1000 kg/m^3), g is the gravitational constant (9.8 m/s^2), and h is the height differential between the movable water tank and the reference tank, which is at the level of the microscope stage. Panel **f** shows what may occur with a very soft egg, with the cell tether aspirated into the pipette very easily (i.e., with very little aspiration pressure) and very far into the pipette (as indicated by the white arrow)

specific point during MPA when the length of the deformation pulled into the micropipette (L_p) is equal to the pipette radius (R_p), so that $L_p/R_p = 1$ (Fig. 1). This parameter includes contributions from persistent surface tension as well as any residual amount of elastic deformation on the time-frame over which the deformation is imposed.

2 Materials

2.1 Instrumentation for Micropipette Aspiration

Details of the instrumentation system for MPA that we have used have been previously described in a separate Methods in Molecular Biology chapter [27]. In brief, the system is built on an inverted microscope, with live-cell imaging capability for capturing cell deformation during aspiration. The system is equipped with a micromanipulator (e.g., Sutter Instrument Company, MP225) to hold the micropipette, which is connected by tubing to a motorized manometer as described in a Methods in Molecular Biology chapter for another series [27]. For application of aspiration pressure, the Robinson lab designed a simple and affordable system, utilizing two water tanks, with a movable water tank (controlled with a motorized system connected to Compumotor RP240 [Parker Hannifin Corporation; Rohnert Park, CA]) positioned relative to a reference water tank, which is at the level of the microscope stage. When the movable tank is lower than the reference tank, suction is applied on the micropipette. For our studies of mouse oocytes, temperature of the culture medium for T_{eff} measurements is maintained at 32–37 °C with a miniature temperature controller (MTC; Bioscience Tools, San Diego, CA). We refer interested readers to this chapter for further details [27].

2.2 Supplies

1. Micropipettes—We pulled pipettes using thin-wall borosilicate glass tubing (1.0 mm outer diameter, 0.75 mm inner diameter, 10 cm length; Sutter Instrument Company) and a micropipette puller (PMP102 micropipette puller; MicroData Instruments, Woodhaven, NY). For our studies of mouse oocytes, we have used pipettes pulled to a diameter of ~8 μm, then broken on a microforge (MFG-5 Microforge-Grinding Center, MicroData Instruments). The typical diameter of pipettes we have used with oocytes is ~15 μm (range, 12–22 μm), and we have determined that pipette radius over this size range does not alter the measured effective tension. Micropipette needles are also commercially available (World Precision Instruments; Fire-polished Pre-Pulled Glass Pipettes, TIP5TW1), although we have not used these.
2. Culture medium—We frequently use Whitten's medium (109.5 mM NaCl, 4.7 mM KCl, 1.2 mM KH_2PO_4, 1.2 mM $MgSO_4$, 5.5 mM glucose, 0.23 mM pyruvic acid, 4.8 mM lactic

acid hemicalcium salt) supplemented with 7 mM $NaHCO_3$, 15 mM HEPES, and 0.05% polyvinyl alcohol (PVA; catalog #P8136; Sigma-Aldrich; St. Louis MO) [28]. There are several other culture media for mammalian oocytes and embryos as well, as noted in other chapters in this volume. Dibutyryl cAMP (dbcAMP, N6,2′-O-dibutyrladenosine 3′:5′cyclic monophosphate, Na^+ salt; Sigma catalog # D-0627) is included for culture of prophase I oocytes to maintain meiotic arrest [29]; dbcAMP is made up as a 100 mM stock in H_2O, and added to culture medium at a final concentration of 0.25 mM.

3. Solution for removal of the zona pellucida (ZP)—We have performed our MPA studies with ZP-free oocytes, although others have analyzed ZP-intact oocytes [7]. The ZP is soluble in low pH medium. We have used a homemade solution, Acidic MEMCO (116.4 mM NaCl, 5.4 mM KCl, 10 mM HEPES, 1 mM NaH_2PO_4, 0.8 mM $MgSO_4$, pH 1.5 [30]). Acidic Tyrode's solution is a commercially available option (Sigma-Aldrich, Catalog # T1788). There are other methods of ZP removal as well, such as mechanical shearing, and chymotrypsin treatment to induce swelling of the ZP followed by mechanical shearing of the ZP [31].
4. Glass coverslips (#1-24X55; Fisher Scientific; Waltham, MA) adapted with silicon gaskets (JTR8R-2.0/8 × 9mm; Grace Bio-Labs; Bends, OR). This chamber will be filled with culture medium and will hold the oocytes during the MPA procedure.
5. 4′,6-diamidino-2-phenylindole (*DAPI*; catalog #D9542; Sigma-Aldrich), or other cell-permeable DNA-staining dye for labeling the oocyte DNA.

3 Methods

1. Prepare ZP-free oocytes or zygotes according to standard techniques (*see* Subheading 2.2, **step 3**, and also **Note 1**; MPA also has been used on ZP-intact eggs and early zygotes [7].) If desired, oocytes can be loaded with DAPI to label the maternal DNA. Our method is based on what was originally reported for studies of sperm–egg fusion [32], incubating oocytes in culture medium containing 1 μg/mL DAPI for 90 min, followed by washing the oocytes through three drops of culture medium [33]. Alternatively oocytes can be microinjected with mRNA encoding a fluorescently tagged histone (e.g., H2B-mCherry [34, 35]).
2. Prepare a glass coverslip with a silicon gasket, and fill with culture medium, ensuring that the seal of the gasket on the coverslip is tight. Place this on the microscope stage. Load the aspiration pipette with culture medium (as noted in Subheading 2.2, **step 2**,

containing 0.25 mM of dbcAMP for prophase I oocytes, and without dbcAMP for metaphase II eggs or for zygotes). As described briefly in Subheading 2.1 and in detail in [27], the aspiration pipette is connected by tubing to a two-tank system. Aspiration pressure (ΔP) is generated by hydrostatic pressure, and calculated as $\Delta P = \rho gh$, where ρ is the density of water (1000 kg/m^3), g is the gravitational constant (9.8 m/s^2), and h is the height differential between two tanks. The aspiration pipette and the tubing connections for the entire system should be examined to confirm that no air bubbles or leakage are present. The system is calibrated as described in Steps 3.2–3.4 of [27].

3. Transfer oocytes to the imaging chamber on microscope stage. Oocytes can be viewed by DIC, and as needed, also with fluorescence to view the maternal DNA; this is especially useful for measurements of metaphase II eggs, when metaphase II spindle and egg DNA needs to be identified to assess if the pipette is being applied to away from the spindle (known as the microvillar domain in rodent eggs, the region with which sperm interact) or over the spindle (known as the amicrovillar domain in rodent eggs).
4. Orient an individual oocyte with respect to the micropipette held by the micromanipulator (Fig. 1a). Position the pipette against the oocyte surface. Set up time-lapse image acquisition with 5-s intervals. Begin to apply pressure to the oocyte and start image acquisition. Aspiration pressure is gradually increased by lowering the movable tank relative to the reference tank and microscope stage, in 5 mm increments. Record the displacement of the movable tank relative to the fixed, reference tank (in mm of water) for each image during the live-cell imaging. The oocyte will start to deform, with the portion of cell cortex moving into the pipette due to the gradually increasing suction pressure (Fig. 1b, c; with some exceptions, *see* **Note 2**). The goal is to reach the stage at which the tether of the oocyte pulled into the aspiration pipette forms a hemisphere-shaped deformation inside the pipette; the aspiration pressure at which this occurs is the equilibrium pressure, ΔP_c. This entire process is repeated for multiple oocytes over an experimental session.

DIC images are generated into stack files by MetaMorph software (Molecular Devices; Sunnyvale, CA). These stack images are analyzed using ImageJ software (imagej.nih.gov), along with the notes taken during the imaging session of water tank displacement (and thus aspiration pressure, or ΔP) for each frame. Images are analyzed to measure the cell radius (R_c in μm), and for the point at which the radius of the hemisphere-shaped deformation inside the pipette (L_p in μm) equals the radius of the pipette (R_p in μm). Effective cortical tension (T_{eff}) is measured at this specific point during MPA, when $L_p = R_p$ so that $L_p/R_p = 1$ (Fig. 1c);

as noted above, the aspiration pressure at which this occurs is the equilibrium pressure, ΔP_c. These measurements—ΔP_c, R_c, R_p—are used to calculate T_{eff} from the Law of Laplace by the equation: $\Delta P_c = 2T_{eff}(1/R_p - 1/R_c)$ (Fig. 1e). *See* also **Note 3**.

4 Notes

1. MPA also has been used on ZP-intact oocytes and embryos [7]. The measurement obtained would reflect rigidity in the ZP, and perhaps also the underlying oocyte cortex, although the relative contributions of the ZP and cortex to these measurements would be difficult to assess.
2. As we observed with cytochalasin D-treated metaphase II eggs [1], some oocytes could be sucked into the pipette almost immediately, with very little suction pressure (Fig. 1f). Because such oocyte deform under very little aspiration pressure, it is very difficult to identify an aspiration pressure when the cell tether length equals the radius of the pipette ($L_p = R_p$), and thus, to quantify cortical tension in these cases. Nevertheless, these types of cells can be assumed to have very low effective cortical tension.
3. Other mechanical models may be used for analysis of MPA data [5–7, 16, 22, 27, 36, 37].

Acknowledgments

Our work on cortical tension in oocytes has been supported by Grant #HD074773 from the NIH, with related work in the Robinson lab supported by Grant #GM066817 and in the Evans lab by Grant # HD090624. We are especially grateful to Dr. Stephanie Larson and Dr. Hyo Lee, who led the way in the development of this methodology of use with oocytes, with assistance from Dr. Yee-Seir Kee.

References

1. Larson SM, Lee HJ, Hung PH, Matthews LM, Robinson DN, Evans JP (2010) Cortical mechanics and meiosis II completion in mammalian oocytes are mediated by myosin-II and Ezrin-Radixin-Moesin (ERM) proteins. Mol Biol Cell 21:3182–3192
2. Kryzak CA, Moraine MM, Kyle DD, Lee HJ, Cubeñas-Potts C, Robinson DN, Evans JP (2013) Prophase I mouse oocytes are deficient in the ability to respond to fertilization by decreasing membrane receptivity to sperm and establishing a membrane block to polyspermy. Biol Reprod 89:44
3. Evans E, Yeung A (1989) Apparent viscosity and cortical tension of blood granulocytes determined by micropipet aspiration. Biophys J 56:151–160
4. Derganc J, Božic B, Sventina S, Žekš B (2000) Stability analysis of micropipette aspriation of neutrophils. Biophys J 79:153–162

5. Chaigne A, Campillo C, Gov NS, Voituriez R, Azoury J, Umaña-Diaz C, Almonacid M, Queguiner I, Nassoy P, Sykes C, Verlhac M-H, Terret M-E (2013) A soft cortex is essential for asymmetric spindle positioning in mouse oocytes. Nat Cell Biol 15:958–966
6. Chaigne A, Campillo C, Gov NS, Voituriez R, Sykes C, Verlhac MH, Terret ME (2015) A narrow window of cortical tension guides asymmetric spindle positioning in the mouse oocyte. Nat Commun 6:6027
7. Yanez LZ, Han J, Behr BB, Pera RAR, Camarillo DB (2016) Human oocyte developmental potential is predicted by mechanical properties within hours after fertilization. Nat Commun 7:10809
8. Hayashi K, Ogushi S, Kurimoto K, Shimamoto S, Ohta H, Saitou M (2012) Offspring from oocytes derived from in vitro primordial germ cell-like cells in mice. Science 338:971–975
9. Cole KS (1932) Surface forces of the Arbacia egg. J Cell Comp Physiol 1:1–9
10. Cole KS, Michaelis EM (1932) Surface forces of fertilized Arbacia eggs. J Cell Comp Physiol 2:121–126
11. Mitchison JM, Swann MM (1954) The mechanical properties of the cell surface: II. The unfertilized sea-urchin egg. J Exp Biol 31:461–472
12. Mitchison JM, Swann MM (1955) The mechanical properties of the cell surface: III. The sea-urchin egg from fertilization to cleavage. J Exp Biol 32:734–750
13. Hiramoto Y (1976) Mechanical properties of starfish oocytes. Develop Growth Differ 18:205–209
14. Yoneda M (1976) Temperature-dependence of the tension at the surface of sea urchin eggs. Develop Growth Differ 18:387–389
15. Ikeda M, Nemoto S, Yoneda M (1976) Periodic changes in the content of protein bound sulfhydryl groups and tension at the surface of starfish oocyts in correlation with the meiotic division cycle. Develop Growth Differ 18:221–225
16. Reichl EM, Ren Y, Morphew MK, Delannoy M, Effler JC, Girard KD, Divi S, Iglesias PA, Kuo SC, Robinson DN (2008) Interactions between myosin and actin crosslinkers control cytokinesis contractility dynamics and mechanics. Curr Biol 18:471–480
17. Luo T, Mohan K, Iglesias PA, Robinson DN (2013) Molecular mechanisms of cellular mechanosensing. Nat Mater 12:1064–1071
18. Evans JP, Robinson DN (2011) The spatial and mechanical challenges of female meiosis. Mol Reprod Dev 78:769–777
19. Girard KD, Kuo SC, Robinson DN (2006) Dictyostelium myosin II mechanochemistry promotes active behavior of the cortex on long time scales. Proc Natl Acad Sci U S A 103:2103–2108
20. Girard KD, Chaney C, Delannoy M, Kuo SC, Robinson DN (2004) Dynacortin contributes to cortical viscoelasticity and helps define the shape changes of cytokinesis. EMBO J 23:1536–1546
21. Reichl EM, Effler JC, Robinson DN (2005) The stress and strain of cytokinesis. Trends Cell Biol 15:200–206
22. Yang L, Effler JC, Kutscher BL, Sullivan SE, Robinson DN, Iglesias PA (2008) Modeling cellular deformations using the level set formalism. BMC Syst Biol 2:68
23. Reichl EM, Robinson DN (2007) Putting the brakes on cytokinesis with alpha-actinin. Dev Cell 13:460–462
24. Cross SE, Jin Y-S, Rao J, Gimzewski JK (2007) Nanomechanical analysis of cells from cancer patients. Nat Nanotechnol 2:780–783
25. Sun Q, Luo T, Ren Y, Florey O, Shirasawa S, Sasazuki T, Robinson DN, Overholtzer M (2014) Competition between human cells by entosis. Cell Res 24:1299–1310
26. Poirier CC, Ng WP, Robinson DN, Iglesias PA (2012) Deconvolution of the cellular force-generating subsystems that govern cytokinesis furrow ingression. PLoS Comput Biol 8:e1002467
27. Kee YS, Robinson DN (2013) Micropipette aspiration for studying cellular mechanosensory responses and mechanics. Methods Mol Biol 983:367–382
28. Whitten WK (1971) Nutrient requirements for the culture of preimplantation embryos in vitro. Adv Biosci 6:129–139
29. Cho WK, Stern S, Biggers JD (1974) Inhibitory effect of dibutyryl cAMP on mouse oocyte maturation in vitro. J Exp Zool 187:383–386
30. Evans JP, Schultz RM, Kopf GS (1995) Identification and localization of integrin subunits in oocytes and eggs of the mouse. Mol Reprod Dev 40:211–220
31. Evans JP, Kopf GS, Schultz RM (1997) Characterization of the binding of recombinant mouse sperm fertilin β subunit to mouse eggs: evidence for adhesive activity via an egg β_1 integrin-mediated interaction. Dev Biol 187:79–93
32. Conover JC, Gwatkin RBL (1988) Preloading of mouse oocytes with DNA-specific fluorochrome (Hoechst 33342) permits rapid detection of sperm-oocyte fusion. J Reprod Fert 82:681–690

33. McGinnis LA, Lee HJ, Robinson DN, Evans JP (2015) MAPK3/1 (ERK1/2) and myosin light chain kinase in mammalian eggs affect myosin-II function and regulate the metaphase II state in a calcium- and zinc-dependent manner. Biol Reprod 92:146
34. Madgwick S, Hansen DV, Levasseur M, Jackson PK, Jones KT (2006) Mouse Emi2 is required to enter meiosis II by reestablishing cyclin B1 during interkinesis. J Cell Biol 174:791–801
35. Yun Y, Lane SIR, Jones KT (2014) Premature dyad separation in meiosis II is the major segregation error with maternal age in mouse oocytes. Development 141:199–208
36. Hochmuth RM (2000) Micropipet aspiration of living cells. J Biomech 33:15–22
37. Chaigne A, Campillo C, Voituriez R, Gov NS, Sykes C, Verlhac M-H, Terret M-E (2016) F-actin mechanics control spindle centring in the mouse zygote. Nat Commun 7